MECHANICAL PROPERTIES TRANSFORMATION ON $Zr_{54}Al_{17}Co_{29}$ BULK METALLIC GLASS BY PARTIAL CRYSTALLIZATION

Yanuar Rohmat Aji Pradana[1,3], Jason Shian-Ching Jang[1,2], Sofyan Arief Setyabudi[3]
[1]Department of Mechanical Engineering, National Central University, Chung-Li, Taiwan, ROC
[2]Institute of Material Science and Engineering, National Central University, Chung-Li, Taiwan, ROC
[3]Department of Mechanical Engineering, Brawijaya University, Malang, Indonesia
+6285815407963
E-mail: yanuarrohmat@gmail.com

Abstract

Study on biomaterials is recently essential for rapid development of medical application and $Zr_{54}Al_{17}Co_{29}$ BMG becomes promising candidate due to the lack of toxic elements. Partial crystallization by isothermal annealing at SCL region was used to variate the crystallinities of BMG. The structural and thermal properties of as cast and partially crystallized samples were confirmed by XRD and DSC test, while microvickers and compression test were further utilized to investigate their mechanical properties. By the higher crystallinity, the hardness could be slightly increased in range 540 ± 5 to 575 ± 5 H_v. As-cast sample shows the yield strength and plastic strain of 2130 ± 75 MPa and $2.2 \pm 1.6\%$. The yield strength is increased by the presence of 10% nanocrystal, afterwards, fall and raise phenomena are obtained with further crystallinity. However, with higher crystallinity, the plasticity is significantly degraded and no more plastic strain observed at sample with 50% of crystallinity. Both the presence of nanocrystalline phase and free volume annihilation are the reason of mechanical properties change on the Zr-based BMG.

Keywords: *$Zr_{54}Al_{17}Co_{29}$ BMG, partial crystallization, yield strength, plasticity.*

INTRODUCTION

Nowadays, understanding of bulk metallic glasses (BMGs) has attracted a huge attention in materials research due to their unique properties [1, 2]. Zr-based BMGs are widely used for biomaterials, such as bone implant and medical devices, due to their high strength, high wear resistance, low Young's modulus and good biocompatibility [3, 4]. On the other hand, the corrosion resistance is much better than other bases [5]. By the absence of Ni, Cu, Be, as harmful element, Zr-Al-Co BMGs became the promising system for biomaterial. Co is classified as toxic element, but the total mass of Co ions released from glassy state after implantation is lower than that on Co-alloy [6].

However, Zr-Co-Al BMGs suffer on limited plastic strain and restrict their applications [6]. Introducing certain amount of crystalline phases inside the glassy matrix is reported could modify their mechanical properties [7], where, in optimum and homogeneous crystalline content, their limited plastic strain could be overcome. The secondary crystalline phase could act both generate larger nucleation site to increase the shear bands multiplication possibility, and branch the single shear band into several secondary shear bands, so, cathastrophic failure could be delayed [8]. One of the ways to produce the crystalline phase is by annealing the BMG sample at supercooled liquid (SCL) temperature region for certain time, depend on designed degree of crystallinity obtained from DSC analyses.

It is widely known that BMGs have excess free volume, which is defined as voids playing a dominant role in the diffusive arrangement of atom, trapped inside the amorphous structure due to rapid solidification. This free volume also determines the mechanical properties of BMGs [8]. Annealing the glasses at temperature around glass transition temperature (T_g) will annihilate the free volume and relaxed the structure into equilibrium state. Because deformation of BMGs is accommodated by generation of multiple shear bands initiated from free volume as nucleation site, annihilation of these voids will limit shear bands generation and cause embrittlement [9, 10]. Therefore, optimum annealing condition have to be achieved to get the sufficient nanocrystal content and size without significantly reduce the

free volume, thus, mechanical property improvements could be achieved [11]. It is believed as the simplest way to overcome the lack of plasticity on monolithic BMGs.

In present work, both hardness and compression test were performed on as cast and partialy crystallized $Zr_{54}Al_{17}Co_{29}$ BMG samples. This composition has been reported to exhibit high glass forming ability (GFA) [12]. Partially crystallized samples were prepared by isothermal annealing treatment at SCL temperature for different annealing time to investigate the mechanical properties change caused by structural modification on BMG.

EXPERIMENTAL PROCEDURE

Master alloy with nominal atomic composition of $Zr_{54}Al_{17}Co_{29}$ were prepared from the mixture of pure element (>99.9% purity) by arc melting inside Ti-gettered argon atmosphere. All samples were melted at least four times to reach chemical homogeneity. The ingots resulted from previous process were remelted and formed into copper mold by suction casting with diameter of 2 mm.

Thermal analyses of as-cast BMG samples were carried out by Mettler Toledo Differential Scanning Calorimetry (DSC) Instruments. Non-isothermal analysis was utilized to obtain the specific temperature, such as glass transition temperature (T_g) and crystallization temperature (T_x). Subsequently, isothermal DSC analyses were utilized at several temperatures between T_g and T_x to confirm crystallization volume fraction transformed as a function of annealing time curve.

Isothermal annealing was done inside the tubular vacuum furnace at selected temperature for different time depend on designed crystallization contents determined from isothermal analysis curves mentioned above. Afterwards, the structure of as cast and partially crystallized samples was tested using Bruker D8A X-ray Diffraction (XRD) Instruments, Germany with scanning rate of 4.861º/min.

To investigate the mechanical properties of all samples, both microvickers and compression tests were used. Hardness test was done using Mitutoyo Microwizhard Hardness Testing Machine with load of 2 kg. For compression test, the samples having diameter of 2 mm were cut and polished to achieve a height and diameter ratio of 2:1. Room-temperature compression tests were performed on Hung Ta Instrument HT-8503 with a constant strain rate of $1 \times 10^{-4}\,s^{-1}$. Finally, the fracture surfaces were analyzed using FEI Nova Nano Scanning Electron Microscopy (SEM) 230 to check the shear band generation.

RESULTS AND DISCUSSIONS

The glassy structure of as cast $Zr_{54}Al_{17}Co_{29}$ sample was firstly confirmed by XRD pattern performed in **Fig. 1 (inset)**. No crystalline peak observed indicates the rod is fully amorphous. In parallel, DSC curve indicates clear T_g and T_x as shown in **Fig. 1**.
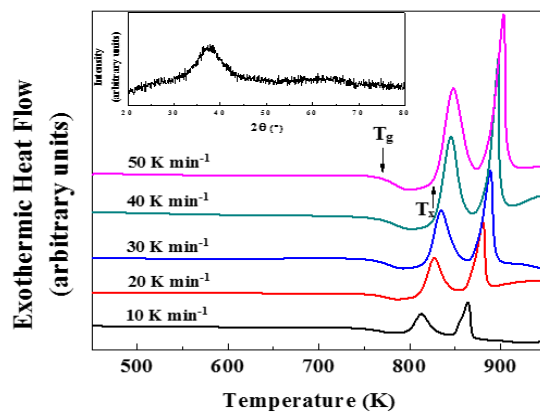
Fig. 1. Non-isothermal DSC curves of $Zr_{54}Al_{17}Co_{29}$ BMG as a function of different heating rates. (Inset: XRD pattern of as cast $Zr_{54}Al_{17}Co_{29}$ BMG)
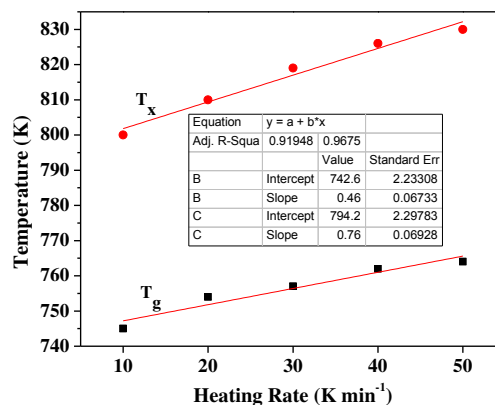
Fig. 2. Linear fitting of of non-isothermal DSC plots as function of different heating rates.

Because these specific temperatures determined by non-isothermal DSC test will shift to higher value at higher heating rate, T_g and T_x are over-estimated and inappropriate for using as isothermal annealing parameter, so real T_g and T_x need to be predicted by extrapolating the data of all heating rate to heating rate of 0 K/min (isothermal). From extrapolating using Origin Pro 8 software, the real T_g and T_x are estimated as 742 and 794 K (**Fig. 2**), therefore, the width of supercooled liquid region ($\Delta T_x = T_x - T_g$) is known as 52 K. From the data mentioned above, as cast $Zr_{54}Al_{17}Co_{29}$ BMG samples were isothermally annealed at three different temperatures within ΔT_x which are 783, 788, and 793 K. By utilizing Johnson-Mehl-Avrami (JMA) isothermal analysis based on following **Eq. (1),** [13]:

$$x(t) = 1 - \exp[-(kt)^n] \qquad (1)$$

where ;
x : crystallinity/volume fraction of crystallization (%)
k : temperature-sensitive factor, [k = k_0 exp($-\beta/RT$), where k_0 is a constant],
n : exponent that reflects the nucleation rate and/or the growth mechanism.
t : annealing time (s)

the crystallinity as the function of annealing time *t* was assumed to be the same as heat released. *x*(*t*) is obtained by integrating the area under the peak of the the curve and dividing with total area.
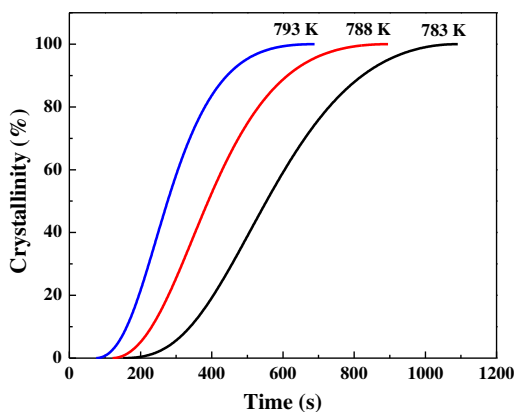

Fig. 3. Crystalline volume fraction transformed as a function of annealing time plots.

The crystallization volume fraction transformed as a function of annealing time plots of the sample are shown on **Fig. 3**. Based on the plots, lower annealing temperature provides larger both of incubation and crystallization time intervals, therefore, 783 K was choosen as temperature reference for annealing the samples.

By varying annealing time on the plot with annealing temperature of 783 K, the designed crystallinity of the samples could be estimated. Annealing time of 0, 341, 405, 459, 507, and 555 s are applied to generate 0 (as cast), 10, 20, 30, 40 and 50% crystallinities.

Fig. 4 shows the XRD patterns of as cast and partially crystallized $Zr_{54}Al_{17}Co_{29}$ BMG samples with 10, 20, 30, 40, and 50% crystallinities. As mentioned before, as cast sample shows single broad peak without crystalline peak observed indicating amorphous nature of this material. The crystalline peak is still not clearly detected at 10 and 20% crystallinity samples. However, 30 and 40% crystallinity samples show the single crystalline peak in the pattern indicating amorphous and nanocrystal phases both exist in these samples, and more crystalline peak appearances are performed at 50% crystallinity sample indicating more nanocrystal content than the other samples. The nanocrystal of 10 and 20 crystallinity sample may be too small to be well detected by XRD analysis.
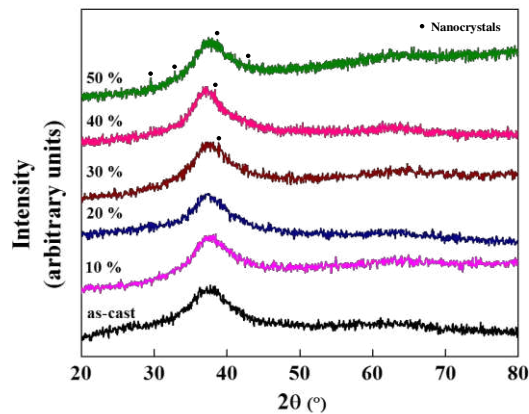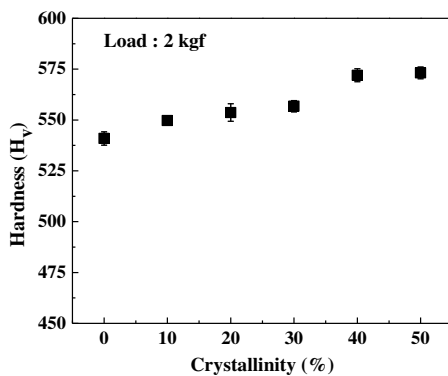

Fig. 4. XRD patterns of as cast and partially crystallized $Zr_{54}Al_{17}Co_{29}$ BMG samples with 10, 20, 30, 40, and 50% crystallinities.

Fig. 5 shows the hardness of as cast and partially crystallized $Zr_{54}Al_{17}Co_{29}$ BMG samples with 10, 20, 30, 40, and 50% crystallinities. The hardness of as cast sample is defined to be 540 $\pm$ 5 H_v. By the presence of nanocrystals, the

hardness is slightly increased and could reach up to 575 ± 5 H_v at sample with 50% crystallinity. The whole hardness data are listed in **Table 1**.

Since nanocrystallization was reached through annealing at temperature above T_g for certain time, the hardness improvement is attributed by both of the precipitation hard intermetallic compounds and free volume annihilation due to thermal energy exposed to BMG sample. Jiang et al (2007), revealed that the free volume has more sensitivity on hardness and elastic modulus than that on plastic flow behavior [14].

Fig. 5. Hardness of as cast and partially crystallized $Zr_{54}Al_{17}Co_{29}$ BMG samples with 10, 20, 30, 40, and 50% crystallinities.

Fig. 6 shows true stress-strain curves of as cast and partially crystallized $Zr_{54}Al_{17}Co_{29}$ BMG samples with 10, 20, 30, 40, and 50% crystallinities. As cast sample generates remarkable yield strength and plastic strain of 2130 ± 75 MPa and $2.2 \pm 1.6\%$. The yield strength is increased by the presence of 10% nanocrystal with 2217 ± 69 MPa, afterwards, fall and raise phenomena are obtained with further crystallinity. The increase of yield strength is mainly caused by the generation of hard intermetallic compounds. While the evolution of yield strength at sample with crystallinity more than 20% are suggested by inhhomogeneously distributed nanocrystals inside the glassy

matrix, which may accumulate localized stress concentration, and finally vary the strength [15].
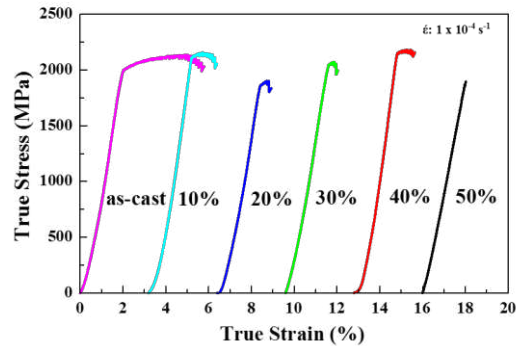
Fig. 6. True stress-strain curves of as cast and partially crystallized $Zr_{54}Al_{17}Co_{29}$ BMG samples with 10, 20, 30, 40, and 50% crystallinities.

In parallel, the plastic strain presents a decreasing trend with the presence of 10% or more nanocrystals. As cast sample shows plastic strain of $2.2 \pm 1.6\%$ and decrease up to $0.3 \pm 0.4\%$ at sample with 40% nanocrystal content. Moreover, no plastic strain observed at sample with 50% crystallinity. This deteroriation may be caused by hard intermetallic compound generation distributed inhomogeneously inside the glassy matrix inducing localized stress concentration [15]. On the other hand, free volume annihilation during annealing process still plays an important role on deformation and control the plastic flow of BMG, especially lower the plasticity, therefore, reduction of free volume has been attributed to the embrittlement [11]. This phenomenon is clearly performed at sample with 50% crystallinity. The plasticity degradation indicates that an optimum nanocrystalline content and critical free volume amount for significant plastic deformation have not been satisfied using current annealing condition. Both yield strength and plastic strain data are also summarized in **Table 1**.

Table 1. Summary of hardness and compression test results on as cast and partially crystallized $Zr_{54}Al_{17}Co_{29}$ BMG samples with 10, 20, 30, 40, and 50% crystallinities.

Crystallinity (%)	H (H$_V$)	σ_y (MPa)	σ_f (MPa)	ε_p (%)
0	540 ± 5	2130 ± 75	1930 ± 130	2.2 ± 1.6
10	550 ± 2	2217 ± 69	2122 ± 122	1.1 ± 0.5
20	554 ± 4	1909 ± 44	1902 ± 71	0.2 ± 0.2
30	559 ± 3	2024 ± 37	1993 ± 6	0.2 ± 0.2
40	572 ± 3	2044 ± 181	2051 ± 187	0.3 ± 0.4
50	575 ± 5	1800 ± 120	1810 ± 120	0

Fig. 7 is presented to evident the fracture surface on the samples. Fig. 7 (a) shows the side view and fracture surface morphology of as cast sample. Dense shear band multiplications are clearly observed indicating the fracture do not through catasthropic mode. Fracture angle forms 45° indicating the high pasticity of material. As cast sample shows typical vein pattern resulted from narrow shear bands propagation. On the other hand, Fig. 7 (b) shows no shear band and only crack traces could be detected from side view of sample with 50% crystallinity. Only brittle morphology could be seen from the fracture surface. It indicates that the deformation is not dominated by glassy matrix. This embrittlement phenomenon is also indicated due to free volume annihilation.
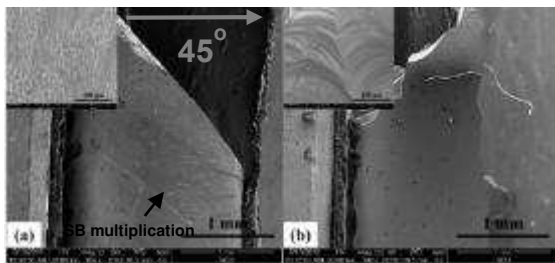
Fig. 7. SEM images of side view on as cast and partially crystallized $Zr_{54}Al_{17}Co_{29}$ BMG samples with 50% crystallinity. (Insets: fracture surface morphologies)

CONCLUSIONS

According to the DSC, XRD, hardness test, compression test, and SEM analysis, the conclusion of this study could be summarized as: $Zr_{54}Al_{17}Co_{29}$ bulk metallic glass is reported having T_g, T_x, and ΔT_x (T_x-T_g) of 742, 794, and 52 K respectively. $Zr_{54}Al_{17}Co_{29}$ bulk metallic glass rods were isothermally annealed to variate their microstructure with different volume fraction nanocrystal contents. By the

increase of crystallinity, the hardnes is slightly improved at range 540 ± 5 H_v of as cast to 575 ± 5 H_v of 50% crystallinity sample. The yield strength and plastic strain of as cast are 2130 ± 75 MPa and 2.2 ± 1.6%. The yield strength is increased by the presence of 10% nanocrystal, afterwards, fall and raise phenomena are obtained with further crystallinity, while improvement of plastic strain is not observed instead of embrittlement, by the presence of nanocrystals. Hard intermetallics precipited during isothermal annealing and free volume annihilation play an important rule to change the mechanical properties of partially crystallized BMG.

REFERENCES

[1] Inoue, A., 2000. Stabilization of Metallic Supercooled Liquid and Bulk Amorphous Alloys. *Acta Materialia*, 48, pp.279–306.

[2] Huang, J.C., Chu, J.P. and Jang, J.S.C., 2009. Recent progress in metallic glasses in Taiwan. *Intermetallics*, 17(12), pp.973–987.

[3] Niinomi, M., Nakai, M., and Hieda, J., 2012. Development of new metallic alloys for biomedical applications. *Acta Biomaterialia*, 8, pp. 3888–3903.

[4] Hua, N., Huang, L., He, W., Pan, S., and Zhang, T., 2013. A Ni-free high-zirconium-based bulk metallic glass with enhanced plasticity and biocompatibility. *Journal of Non-Crystalline Solids*, 376, pp.133–138.

[5] Guan, B., Shi, X., Dan, Z., Xie, G., Niinomi, M., and Qin, F., 2016. Corrosion behavior, mechanical properties and cell cytotoxity of Zr-based bulk metallic glasses. *Intermetallics*, 72, pp.69–75.

[6] Wada, T. Qin, F. X., Wang, X. M., Yoshimura, M., Inoue, A., Sugiyama, N., Ito, R., and Matsushita, N., 2009. Formation and bioactivation of Zr-Al-Co

bulk metallic glasses. *Journal of Materials Research*, 24(9), pp.2941–2948.

[7] Hajlaoui, K., Yavari, A. R., LeMoulec, A., Botta, W. J., Vaughan, F. G., Das, J., Greer, A. L., and Kvick, Å., 2007. Plasticity induced by nanoparticle dispersions in bulk metallic glasses. *Journal of Non-Crystalline Solids*, 353(3), pp. 327–331.

[8] Schuh, C. A., Hufnagel, T. C., and Ramamurty, U., 2007. Mechanical behavior of amorphous alloys. *Acta Materialia*, 55(12), pp. 4067–4109.

[9] Murali, P. and Ramamurty, U., 2005. Embrittlement of a bulk metallic glass due to sub-Tg annealing. *Acta Materialia*, 53(5), pp. 1467–1478.

[10] Kumar, G., Rector, D., Conner, R. D., and Schroers, J., 2009. Embrittlement of Zr-based bulk metallic glasses. *Acta Materialia*, 57(12), pp. 3572–3583.

[11] Mondal, K., Ohkubo, T., Toyama, T., Nagai, Y., Hasegawa, M., and Hono, K., 2008. The effect of nanocrystallization and free volume on the room temperature plasticity of Zr-based bulk metallic glasses. *Acta Materialia*, 56(18), pp. 5329–5339.

[12] Li, T. H., Hsu, K. T., Tsai, P. H., Jang, J. S. C., and Huang, J. C., 2016. Effect of the multiple-metastable crystalline phases on predicting the glass forming ability of ZrAlCo amorphous metallic alloys. unpublished.

[13] Suryanarayana, C. and Inoue, A., 2011. Bulk Metallic Glasses. Taylor and Francis Group, FL: CRC Press.

[14] Jiang, W. H., Liu, F. X., Choo, H., and Liaw, P. K., 2007. Effect of structural relaxation on mechanical behavior of a Zr-based bulk-metallic glass. *Materials Transactions*, 48(7), pp. 1781–1784.

[15] Hsiao, Z. W., Fu, C. C., Tsai, P. H., Jang, J. S. C., Jian, S. R., and Huang, J. C., 2010. Effect of nano-crystallization on the mechanical properties of the $(Zr_{53}Cu_{30}Ni_9Al_8)_{99.5}Si_{0.5}$ bulk metallic glass. *Materials Science Forum*, 638-642, pp. 2933-2937.